Computer Methods and Programs in Biomedicine 224 (2022) 106991

Contents lists available at ScienceDirect

Computer Methods and Programs in Biomedicine

journal homepage: www.elsevier.com/locate/cmpb

Evaluation of optical tracking and augmented reality for needle navigation in sacral nerve stimulation

Rafael Moreta-Martínez[a,b], Inés Rubio-Pérez[c], Mónica García-Sevilla[a,b], Laura García-Elcano[a,d], Javier Pascau[a,b,*]

[a] Departamento de Bioingeniería e Ingeniería Aeroespacial, Universidad Carlos III de Madrid, Leganés 28911, Spain
[b] Instituto de Investigación Sanitaria Gregorio Marañón, Madrid 28007, Spain
[c] Servicio de Cirugía General, Hospital Universitario La Paz, Madrid 28046, Spain
[d] Centro de Investigación Médica Aplicada, Clínica Universidad de Navarra, Madrid 28027, Spain

ARTICLE INFO

Article history:
Received 1 February 2022
Revised 10 June 2022
Accepted 28 June 2022

Keywords:
Surgical navigation
Sacral nerve stimulation
Needle guidance
Augmented reality
Tracking systems

ABSTRACT

Background and objective: Sacral nerve stimulation (SNS) is a minimally invasive procedure where an electrode lead is implanted through the sacral foramina to stimulate the nerve modulating colonic and urinary functions. One of the most crucial steps in SNS procedures is the placement of the tined lead close to the sacral nerve. However, needle insertion is very challenging for surgeons. Several x-ray projections are required to interpret the needle position correctly. In many cases, multiple punctures are needed, causing an increase in surgical time and patient's discomfort and pain. In this work we propose and evaluate two different navigation systems to guide electrode placement in SNS surgeries designed to reduce surgical time, minimize patient discomfort and improve surgical outcomes.

Methods: We developed, for the first alternative, an open-source navigation software to guide electrode placement by real-time needle tracking with an optical tracking system (OTS). In the second method, we present a smartphone-based AR application that displays virtual guidance elements directly on the affected area, using a 3D printed reference marker placed on the patient. This guidance facilitates needle insertion with a predefined trajectory. Both techniques were evaluated to determine which one obtained better results than the current surgical procedure. To compare the proposals with the clinical method, we developed an x-ray software tool that calculates a digitally reconstructed radiograph, simulating the fluoroscopy acquisitions during the procedure. Twelve physicians (inexperienced and experienced users) performed needle insertions through several specific targets to evaluate the alternative SNS guidance methods on a realistic patient-based phantom.

Results: With each navigation solution, we observed that users took less average time to complete each insertion (36.83 s and 44.43 s for the OTS and AR methods, respectively) and needed fewer average punctures to reach the target (1.23 and 1.96 for the OTS and AR methods respectively) than following the standard clinical method (189.28 s and 3.65 punctures).

Conclusions: To conclude, we have shown two navigation alternatives that could improve surgical outcome by significantly reducing needle insertions, surgical time and patient's pain in SNS procedures. We believe that these solutions are feasible to train surgeons and even replace current SNS clinical procedures.

1. Introduction

Sacral neuromodulation or sacral nerve stimulation (SNS) is a minimally invasive procedure where an electrode lead is implanted through the sacral foramina to stimulate the nerve modulating colonic and urinary functions [1]. SNS has been considered a valid alternative during the past two decades when conventional treatments have failed in treating bowel dysfunction pathologies [2].

Abbreviations: AR, Augmented Reality; CT, Computed Tomography; DRR, Direct Reconstruction Radiograph; OTS, Optical Tracking System; SNS, Sacral Nerve Stimulation.

* Corresponding author at: Universidad Carlos III de Madrid, Avenida de la Universidad 30, Leganés 28911, Madrid, Spain.
E-mail address: jpascau@ing.uc3m.es (J. Pascau).

https://doi.org/10.1016/j.cmpb.2022.106991

This practice has shown to be efficient when treating fecal incontinence [3], refractory overactive bladder [4], urinary retention [5], or constipation [6].

One of the most crucial steps in SNS procedures is the placement of the tined lead close to the sacral nerve, as the final position of the electrode will determine the efficacy of the treatment. In order to reach the sacral nerve, a needle is inserted through the posterior sacral foramina S3 or S4, which are usually smaller than 12 × 8 mm [7]. Currently, surgeons perform a combination of visual inspection to localize bony landmarks [8,9] and conventional x-ray fluoroscopy (anterior and lateral projections) to find the target sacral foramen, decide the initial insertion trajectory, and verify the location of the needle with respect to the sacrum while positioning the lead in place [10]. However, needle insertion is very challenging for surgeons. Several x-ray projections are required to interpret the needle position correctly. In many cases, multiple punctures are needed, causing an increase in surgical time and patient's discomfort and pain, not to mention that the lack of reference points in patients with anatomical sacral abnormalities may increase surgical difficulties.

Intraoperative computed tomography (CT) imaging has been previously proposed to estimate the final position of the needle in patients with abnormal sacrum where fluoroscopy has failed [11,12]. Others have combined CT scans inside the operating room with navigation systems to track the position of the needle in real-time, guiding electrode placement, reducing procedural time, and improving surgical outcomes [13,14]. Nonetheless, these techniques have been used in a small number of cases, only when required to perform a complex surgical procedure correctly. Additionally, these systems involved an intraoperative CT, which implies additional radiation exposure to both patients and medical professionals during the intervention, restricting their integration in the clinical practice [15].

As an alternative, patient-specific 3D printed navigation templates have been proposed for accurate electrode lead placement, using a preoperative CT scan to define needle trajectory and perform patient registration [16,17]. However, this solution is limited by the long manufacturing time of the template, the displacement of registration markers during the procedure, resulting in a low registration accuracy, and modifications of the final position of the electrode lead once the template is removed. Finally, Rubio-Perez et al. have presented an alternative application of 3D printing for fabricating patient-specific sacrum biomodels to understand possible patient's anatomy anomalies before surgery [18].

Needle insertion guidance with tracking systems has been applied in surgical procedures such as radiofrequency ablation [19,20] or spine surgery [21]. All these navigation systems provided successful needle guidance. Nevertheless, the navigation information is displayed on external screens, requiring the surgeon to divert his attention from the patient. In this context, augmented reality (AR) technology could provide the surgeon with real-time navigation information directly overlaid in the surgical field [22,23]. Hecht et al. proposed a smartphone-based AR navigation system to display the needle trajectory in the target area for ablation and biopsy procedures, demonstrating a superior needle insertion accuracy compared to CT-guided freehand methods [24]. Besides, Kuzhagaliyev et al. presented the combination of an AR head-mounted display with optical tracking to guide the needle ablation during irreversible electroporation in the pancreas [25].

Although these navigation technologies can improve needle guidance, they have not been implemented in SNS procedures yet. In the past, our group developed an open-source navigation software to track the needle position with respect to the patient in real-time using an electromagnetic tracking system (EMTS) [26]. The proposed solution did not require an intraoperative CT for registration, providing accurate needle guidance for SNS. Nonetheless, the proposal showed several limitations: navigation software did not indicate the target depth, and the EMTS components required asepsis and were affected by metal distortions from other surgical tools.

In this work, we propose and evaluate two different navigation systems to guide electrode placement in SNS surgeries designed to reduce surgical time, minimize patient discomfort and improve surgical outcomes. For the first alternative, we developed an open-source navigation software to guide electrode placement by real-time needle tracking with an optical tracking system (OTS). In the second method, we introduce a smartphone-based AR application that displays virtual guidance elements directly on the affected area, using a 3D printed reference marker placed on the patient, facilitating needle insertion with a predefined trajectory. Both techniques were evaluated to determine which one obtained better results than the current surgical procedure regarding number of insertions, accuracy, time, and radiation exposure. An important contribution is the comparison of both proposals with the clinical method in the same setup. For this purpose, we developed an x-ray software tool to simulate the clinical procedure that calculates direct reconstruction radiographs (DRR), simulating the fluoroscopy acquisitions during the clinical procedure. All methods were evaluated by twelve physicians (inexperienced and experienced users) on a realistic anthropomorphic phantom based on a patient that underwent an SNS procedure. Additionally, our freely available open-source approach will facilitate surgeons' training in these complex procedures, which is currently limited to theoretical lectures and animal experiments.

2. Materials and methods

2.1. Sacral Phantom

We evaluated the proposed surgical navigation systems on a phantom based on a patient suffering from a bowel dysfunction that underwent an SNS procedure. The patient had a standard sacrum shape, with average sacral foramina sizes. This study was performed in accordance with the principles of the 1964 Declaration of Helsinki as revised in 2013. The anonymized patient data and pictures included in this paper are used after written informed consent was obtained from the participant and/or their legal representative, in which he/she approved the use of this data for dissemination activities, including scientific publications.

A preoperative sacral CT scan (Fig. 1a), obtained with the patient in prone position, was used as a template to manufacture an anthropomorphic phantom. The fabricated phantom was composed of two parts: bone and soft tissue (Fig. 1e). The bone structure was 3D printed in polylactic acid (PLA) (Fig. 1c). We included six conical holes (Ø 4 mm x 3 mm depth) on the bone model surface to perform a point-based registration. The part that mimics the soft tissue was designed to have two silicone layers (representing skin and fat tissue), allowing realistic feedback during needle insertion (Fig. 1d).

2.2. Experimental setup

For the three proposed methodologies, a common scenario was set up to perform the validation experiment. Polaris Spectra (Northern Digital Inc. [NDI], Waterloo, ON, Canada) optical tracking system (Fig. 2a) provided real-time tool tracking during the experiment. This OTS presents similar features to commercial alternatives such as Medtronic Stealthstation (Medtronic PLC, Fridley, Minnesota, USA). The tracking device transferred the positioning data to the navigation software using PLUS-Toolkit [27] and OpenIGTLink communication protocol [28].

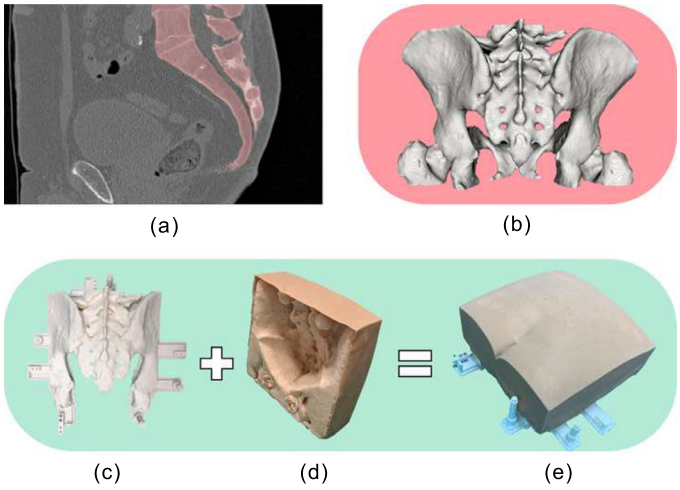

Fig. 1. Images of the patient's anatomy used in this study and the manufactured phantom: (a) Computed tomography coronal slice image, with segmented bone in red; (b) Virtual three dimensional (3D) model of the pelvic bone structures; (c) 3D printed bone in polylactic acid (PLA); (d) Soft tissue in silicone; (c) Phantom assembled.

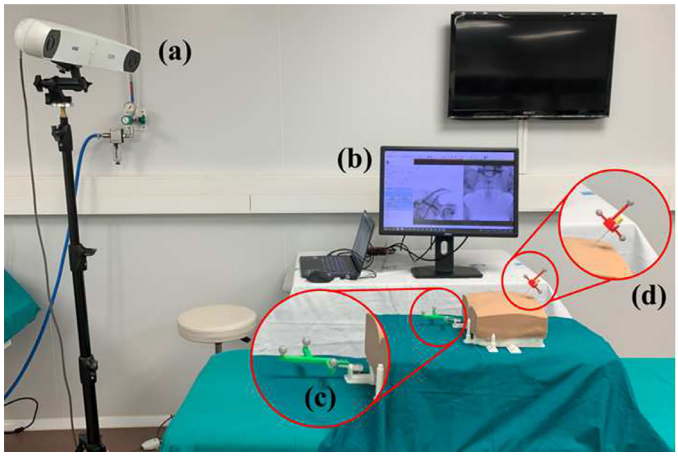

Fig. 2. Experiment setup. (a) Optical tracking device. (b) External display. (c) Optical marker with spherical markers attached to the phantom. (d) Needle with optical markers attached.

A specific optical marker configuration was attached to the phantom (Fig. 2c) to compensate for any possible movement during the experiment. The needle used during the experiment was part of a demonstration surgical kit from Medtronic (Model 3550-18/042294 Lead Introducer Kit, Medtronic PLC, Fridley, Minnesota, USA). We developed a customized 3D printed cap holder with a specific optical marker configuration for the needle (Fig. 2d). Pivot calibration [29] procedure was performed to calculate the relationship between the optical marker attached to the needle and its tip. During the experiment, the needle and the phantom were always tracked, and the position given by the tracking system was used as a gold standard to compare with each navigation method.

2.3. Simulation of the clinical method

A specific software application named *SNS Clinical Simulation* was developed as an extension module in 3D Slicer to simulate current SNS surgical procedures on the manufactured phantom. In this simulation, the objective is to reach the target foramen by inserting the needle using simulated x-ray projections for guidance.

The software allows reproducing realistic anterior and lateral x-ray projections from anatomical structures of the phantom almost instantaneously. In order to create the x-ray projection, a digitally reconstructed radiograph (DRR) algorithm is applied on the CT of the patient from which the phantom was developed. The DRR program receives the CT image and the desired position for the x-ray tube focal point, calculating a projection by bilinear interpolation [30]. To display the needle in the projection, we designed a virtual 3D needle model that is converted to a mask on the CT image coordinate system in its actual position, modifying the corresponding Hounsfield Units (HU) to metallic material (1500 HU). The software steps are summarized as follows:

1. Pivot calibration of the needle for virtual model registration.
2. Selection of the orientation for the projection.
3. Recording of needle position with respect to the phantom.
4. Creation of the virtual 3D needle model mask in phantom CT image coordinate system, modifying the corresponding pixel values to 1500 HU.
5. DRR algorithm execution and projection simulation.
6. Simulated x-ray projection visualization on the user interface.

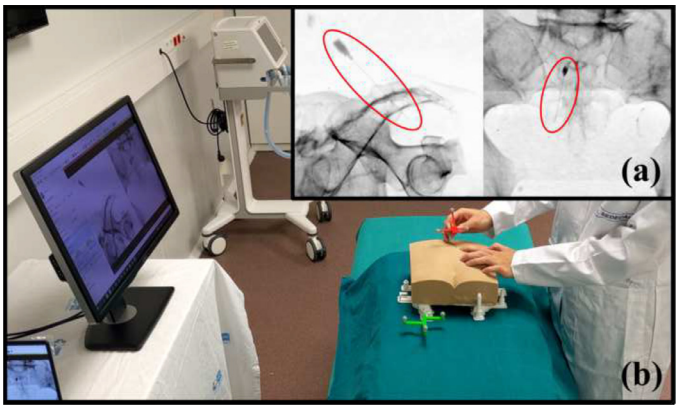

Fig. 3. User performing the clinical method simulation (Video 1). (a) Lateral (left) and anterior (right) simulated projections with the needle circled in red. (b) User inserting the needle into the phantom.

Fig. 3a shows the software user interface, the phantom with the needle inserted in a target position, and the simulated lateral (left) and anterior (right) projections. Video 1 shows a user performing the clinical method simulation.

The source code of *SNS Clinical Simulation* is available on a public GitHub repository at https://github.com/BIIG-UC3M/SacralNerveStimulationSimulationOpen. It can be easily installed as a Python extension module in 3D Slicer version 4.11 or older. Additionally, a CT scan and the 3D models needed for the simulation are available within the repository.

2.4. Surgical navigation with optical tracking system

A software application named *SNSNavigation* was developed as an extension module in 3D Slicer to facilitate needle insertion in SNS procedures. This software has been adapted from López-Velázquez et. al. [26]. NDI tracker transfers the position of the needle and the patient to the software in real-time. *SNSNavigation* software displays the information on an external screen. First, the virtual 3D models of the patient are loaded on the navigation software in the correct orientation. Then, once the target is selected, virtual models are displayed to visualize the trajectory of the needle and the target area. The software divides the screen into two sections to facilitate the guidance process, showing on the left a lateral view and an anterior view of the virtual 3D models on the right (Fig. 4a). The needle is represented as a cylinder with a sphere on the tip. The trajectory of the needle is displayed as a red line with a sphere of Ø 2 mm representing the target point in

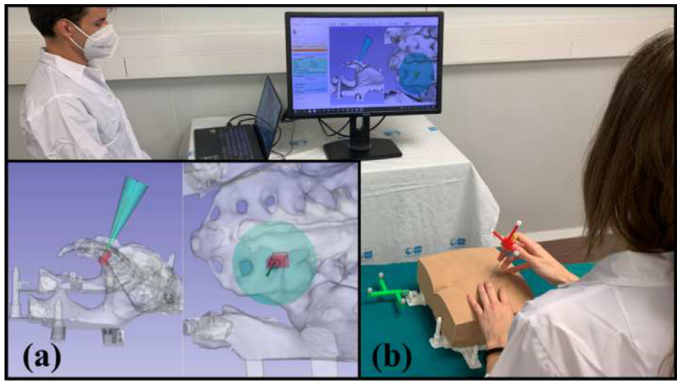

Fig. 4. User performing needle insertion with optical tracking system (OTS) navigation guidance (Video 2). (a) Lateral view (left) and anterior view (right) on the navigation software. Green model represents the trajectory, red model indicates that the tip of the needle is in the target position. The needle is represented with an orange virtual line model. (b) User inserting the needle on the phantom.

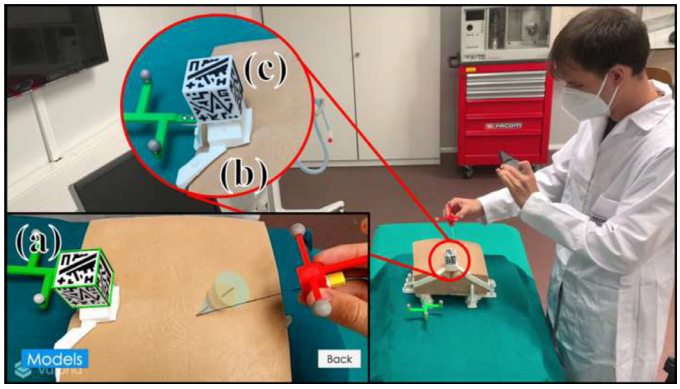

Fig. 5. User performing needle insertion with augmented reality (AR) navigation (Video 3). (a) AR visualization on the smartphone during guidance. (b) Three-dimensional (3D) printed marker adaptor. (c) 3D printed cubic reference marker.

the foramen. The anterior view plane is oriented perpendicularly to the trajectory line. A transparent green virtual model representing the target volume indicates the expected final position. This model corresponds to the shape of the foramen hole, similar to a cylinder with the diameter of the foramen size and between 1 and 2 cm of length (depending on the foramen size). If the needle tip touches this target volume, the model will turn red, indicating that the needle has reached the target position. Additionally, the *SNSNavigation* software can calculate the real-time distance from the needle tip to the target point. Video 2 shows a user performing needle insertion using this OTS navigation guidance.

2.5. Surgical navigation with augmented reality

We developed a smartphone AR application named *SacralNSAR* on Unity platform (version 2019.3) compatible with Android and iOS devices. This video see-through (VST) AR application uses Vuforia software development kit (SDK) (Parametric Technology Corporation Inc., Boston, MA, USA) to detect and track the position of a 3D printed cubic reference marker (30 × 30 × 30 mm) with unique black-and-white patterns on each face (Fig. 5c) [31]. Once the marker is detected on the smartphone camera field of view, the virtual models are displayed overlaid on the real-world image in real-time.

Before navigation, the app presents a menu to select the predefined target and trajectory. Once chosen, virtual 3D models are displayed on the AR screen: the sacral bone, the optimal trajectory to reach the selected sacral foramen, the insertion point on the surface of the phantom, and the target needle insertion depth (Fig. 5a).

The AR reference cube phantom (Fig. 5c) was fixed to a 3D printed adaptor on top of the phantom (Fig. 5b), in the superior area of the gluteus. To know the position of this marker with respect to the phantom, we performed a point-based registration, obtaining the location of the conical holes designed on the marker adaptor surface with the optical tracking system. Then, this registration transformation was transferred and updated on the smartphone (Google Pixel 4 XL, Alphabet Inc., USA). Additionally, a 3D Slicer module was developed to track the position of the needle in real-time to verify if the needle was in the correct target during the experiment. Video 3 represents a user performing the experiment using the AR navigation.

2.6. Evaluation of the navigation alternatives

Needle insertion performance was evaluated using the proposed phantom to compare the current SNS procedure with the two proposed navigation methods: optical tracking system and AR technology.

Twelve volunteers, physicians from the general surgery department at Hospital Universitario la Paz (Madrid, Spain), participated in the experiment. Five of them were attending physicians, and seven medical residents. Of the whole group, seven had prior experience in SNS procedures (experienced users), while the rest were only familiar with the technique (unexperienced users). None of them had previously performed the procedure as primary surgeons, neither had prior experience with navigation systems.

Each volunteer followed the three navigation methods in random order. For each method, we defined the same four targets (S3 Left, S3 Right, S4 Left, and S4 Right) to be found by each participant inserting the needle with a predefined angle and direction. For each method and user, the target order was decided randomly to control for possible effects of the sequencing. Prior to the experiment, an instructor explained each method and gave time ($<$ 15 min) for the participants to familiarize themselves with the system before performing the predefined insertions. The trajectories used for training were not the same as the ones used for the examination. All the operators started with the needle in the same position on the experiment table. The insertion finished once the needle reached the target volume. Each time the user thought that the needle was in the target position, the actual location was obtained from the optical tracking system to check if it was correct. For the clinical method, no trajectory was predefined as physicians performed the procedure following the standard surgical practice. Several metrics were recorded during each intervention: repetition total time, number of punctures (a new puncture was considered if the needle was extracted from the phantom soft tissue and inserted again), time per puncture, number of stimulations and number of x-ray projections.

2.6.1. Statistical analysis

Statistical analysis was conducted using Python 3.7 and SciPy libraries [32]. Mann Whitney U test was used when two groups were compared. Kruskal-Wallis test was applied when comparing more than two variables, with Conover-Iman test as post hoc analysis between groups. Differences were considered to be statistically significant for p-values $<$0.05. Results of the Mann Whitney U and Kruskal-Wallis tests are reported as medians, interquartile ranges (IQR) and associated p-values.

Table 1
Median and interquartile range (in brackets) for the evaluated metrics in all experiments grouped by guidance method.

Parameter	Clinical Method	OTS Method	AR Method	p-value
Total Time [s]	106.64 [73.40 - 215.12]	32.26 [24.12 - 56.71]	53.29 [35.73 - 94.52]	$< 0.001^*$
Number of Punctures	2.0 [1.0 - 4.0]	1.0 [1.0 - 1.0]	1.0 [1.0 - 2.0]	$< 0.001^*$
Time/Puncture [s/puncture]	51.82 [37.05 - 77.85]	30.65 [24.12 - 44.05]	41.67 [31.50 - 52.82]	$< 0.001^*$
Number of Stimulations	3.0 [1.0 - 7.0]	1.0 [1.0 - 1.0]	1.0 [1.0 - 2.0]	$< 0.001^*$

Table 2
Median and interquartile range (in brackets) for the evaluated metrics grouped by method (clinical and optical tracking system navigation) and type of user (inexperienced and experienced).

Method	Parameter	Inexperienced	Experienced	p-value
Clinical	**Total Time [s]**	77.29 [68.47 - 154.00]	148.56 [80.51 - 234.19]	0.076
	Number of Punctures	1.0 [1.0 - 2.0]	3.0 [1.0 - 5.25]	**0.036***
	Time/puncture [s/puncture]	65.59 [44.16 - 85.59]	47.28 [27.86 - 77.07]	0.062
	Number of Stimulations	1.0 [1.0 - 4.0]	4.5 [2.0 - 7.5]	**0.029***
Optical Tracking System Navigation	**Total Time [s]**	29.18 [19.92 - 34.95]	43.25 [27.53 - 67.37]	**0.021***
	Number of Punctures	1.0 [1.0 - 1.0]	1.0 [1.0 - 1.0]	0.226
	Time/puncture [s/puncture]	27.92 [19.92 - 33.03]	31.69 [27.53 - 49.84]	**0.033***
	Number of Stimulations	1.0 [1.0 - 1.0]	1.0 [1.0 - 1.0]	0.337

3. Results

Table 1 represents the medians and interquartile range (IQR) obtained from the different experiments and metrics for the three evaluated methods. The median [IQR] time for the physicians was 106.64 [73.4–215.12] s with the clinical approach. In comparison, the navigation methods reduced the total time by 3 or 2 times using OTS (32.26 [24.12 - 56.71] s) and AR (53.29 [35.73 - 94.52] s) navigation systems, respectively. Moreover, concerning the number of punctures needed to reach the target, the physicians needed 1 insertion in most cases to reach the foramen when using the OTS navigation, and 1 or 2 insertions when using the AR method. In contrast, performing the simulated clinical SNS procedure, users inserted the needle 2.0 [1.0 to 4.0] times to reach the foramen. Additionally, operators spent more time per puncture when inserting the needle with the AR system than with the OTS device. For all the metrics, the Kruskal Wallis test showed a significant difference between all methods with a p-value <0.001. Then, the Conover-Imann post hoc analysis demonstrated that there was a significant difference comparing each method against each other.

Furthermore, for the traditional method, the participants required an average of 10.71 ($\pm$ 8.86) projections to complete the task. This value indicates that the radiation exposure to the patient would have been 6.4 (mSv) if we estimate that each projection radiates 0.6 mSv [34]. No x-ray projections would be needed when using the proposed navigation systems while navigating the needle.

When comparing metrics grouping the results by target, we did not see any significant difference, except when using the AR method. Fig. 6a and 6b show the distribution of the total time and number of punctures, respectively, when the operators performed the task with AR guidance. Each boxplot shows three different grouping criteria: on the left, by target foramen (S3L, S3R, S4L, S4R), on the center, by distance from the operator (close, C; far, F) and on the right, by foramen sacral location (S3, S4). The distribution demonstrates that the physicians performed significantly worse (p-value <0.05) when the foramina were farther away in both metrics.

When comparing the different metrics grouped by the hierarchy of the physician (residents vs. attending physicians), we did not find any significant difference. However, we found different results between inexperienced and experienced users. Table 2 presents the results separated by method and type of user (experienced and inexperienced). Focusing on the clinical method, we found that inexperienced users inserted the needle significantly fewer times (1.0, [1.0 - 2.0]) compared to experienced users (3.0, [1.0 - 5.25]). This probably means that experienced users prefer to repeat the insertion and not rummage in the patient while the needle is inserted. Looking at the OTS method, we found that experienced users took significantly longer times to perform the task ($p < 0.05$). This is an unexpected finding that may indicate that experienced users prefer to take their time to obtain a successful result, trying to avoid unnecessary harm to patients while performing the insertion.

4. Discussion

In this study we have presented and evaluated two alternative surgical navigation systems to guide electrode placement in SNS procedures. Our objectives were to reduce surgical time, minimize patient discomfort and improve surgical outcomes. The first proposal is based on optical tracking to guide needle insertion, while the second alternative presents a smartphone-based AR system to virtually superimpose the planned trajectory on the surface of the patient. We have also developed an x-ray simulator to compare our navigation solutions with the clinical method. The feasibility of the proposed systems has been evaluated by clinical users on a realistic anthropomorphic phantom.

The main novelty of this study is not only the proposal of alternative navigation solutions for SNS, but also the extensive comparison with the current clinical method, on the same setup, through metrics that could impact the clinical procedure. Open-source software allowed us to respond to the needs of this surgical procedure, maximizing usability. Commercially available navigation systems, such as Medtronic Stealthsatation, have previously been used in SNS [13]. However, they present several limitations that restrict daily clinical implementation, including a complex registration procedure or limited needle trajectory visualization. Philips ClarifEye (Philips N.V., Eindhoven, Netherlands) offers AR guidance for tool insertion in spinal surgery [33]. This solution is not adapted to SNS, requires several CT acquisitions, and visualizes AR information on an external screen.

During the evaluation of the proposal, twelve physicians performed a total of 144 needle insertions. With this experiment, we have compared both navigation alternatives with the clinical method in terms of number of punctures and time to complete the task. From these metrics, we can observe that users performing any of the proposed navigation solutions took less time to complete each insertion, needed fewer punctures to reach the tar-

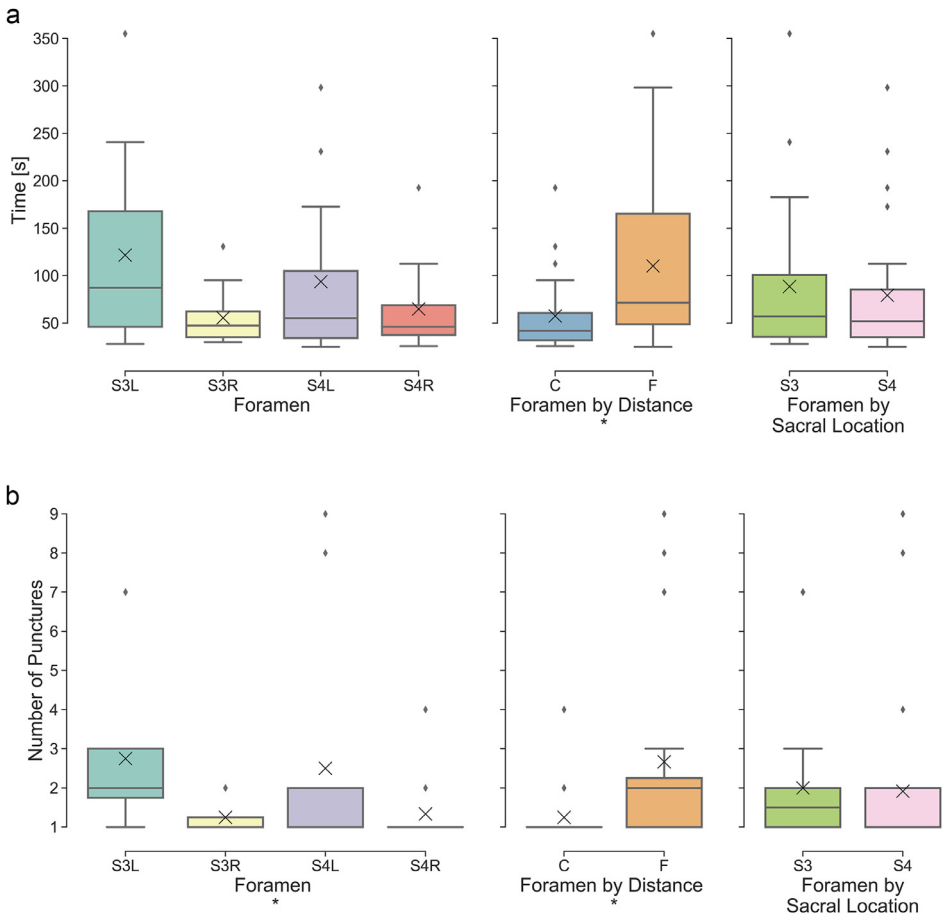

Fig. 6. Boxplots from experiments where physicians performed the needle insertion with AR guidance. The results are grouped by the target foramen (S3 Left -S3L-,S3 Right -S3R-, S4 Left -S4L-, S4 Right -S4R-), target distance (close -C- and far -F-), and target sacral foramen (S3 and S4) in left, center and right plots respectively. (a) Shows the time needed to perform the task. (b) Shows number of punctures needed to reach the target. The horizontal line inside the box represents the median and the cross the mean of each data set. (*) indicates significant ($p < 0.05$) statistical differences.

get, spent less time per puncture and needed a smaller number of stimulations, compared with the clinical method. Additionally, the results achieved from the navigation solutions in terms of average number of punctures (1.23 ± 0.59 and 1.96 ± 1.90 for the OTS and AR methods respectively) and mean puncture time (36.83 ± 20.40 s and 44.43 ± 17.53 s for the OTS and AR methods respectively) are comparable with the ones found in the literature that used alternative navigation procedures in patients, obtaining similar values for number of punctures (1.5 ± 0.7) and mean puncture time (246 ± 132 s)[1] [16]. Our solutions could improve surgical outcomes and reduce patient pain and discomfort during surgery.

The augmented reality alternative uses a smartphone to display virtual elements overlaid on the patient. It might seem that the need to hold the device with one hand might not be the best option in a surgical scenario, since surgeons usually require the use of both hands continuously. Nevertheless, our previous experience showed an enormous potential of using the smartphone as a surgical navigation device, due to high navigation precision and a convenient setup in the operating room with a sterile bag or cover [35–37]. Additionally, results from the experiment showed that AR improved the metrics compared to the clinical method. Nevertheless, depth perception and registration are limiting factors in AR for needle guidance. Participants needed significantly more punctures and total time to reach the farthest away target foramina. This can be explained by the difficulty in orienting the smartphone to correctly visualize the trajectory line perpendicular to the needle insertion point. This problem increases with the distance from the user, as can be observed in Fig. 5, and produced a displacement of the needle trajectory when it was inserted. Additionally, marker-based registration is still a nuisance, as the marker always needs to be visible, frustrating users when the detection fails. As an alternative, surface recognition could be a solution to this problem, but accuracy results are still far from those obtained with marker-based registration [38].

Looking into the future, head-mounted displays (HMD), such as Microsoft HoloLens 2 [39], Magic Leap 1 (Plantation, Magic Leap, FL, USA) [40], or xvision system (Augmedics, Chicago, IL, USA) [41],could be the perfect hands-free AR alternative. This device recognizes hand gestures and voice commands to control the user interface, overcoming the main limitations of the smartphone as AR device. Recent studies have proposed HMD for surgical [42,43] or needle guidance [44]. However, registration, depth perception, and spatial awareness are still significant drawbacks in clinical practice. In our case, the main reason restricting the use of HoloLens for needle navigation was the limited tracking capability with Vuforia and small 3D markers like the cube we used. A large marker, such as that proposed in [45], is not practical in real clinical scenarios. On the other hand, in [46] they propose Magic Leap 1 for guidance in percutaneous punctures. Their registration requires both intra-operative CT and optical tracking. An alternative to avoid optical

[1] Table 1 shows medians and interquartile range since data did not follow a normal distribution. We calculated means and standard deviations from our original data to allow comparison with previous literature.

tracking would be calculating the image-to-patient registration between the AR marker and the preoperative CT scan with a surface scan acquired during surgery, as described in [47]. This straightforward solution does not require external devices or instrumentation during navigation.

Although AR seems a promising alternative, participants obtained better results in all the metrics when using the more traditional optical navigation system. Although the need to remove the attention from the phantom, looking away at an external display, could be the main drawback, they still performed better. Indeed, tracking the needle position in real-time helped the surgeons to insert the needle more confidently as depth was continuously reported. This feature could be included in the AR navigation by adding an additional marker to the needle holder [43,48]. However, this reference needs to be large enough to be detected by the AR camera, adding extra weight that could limit the manipulation of the needle. The current state of the art in AR needs improvement, so traditional navigation is still the best solution in the near future.

The navigation solutions proposed present also some limitations. We did not measure the accuracy in terms of distance to target at the end of the needle insertion. The main goal of this surgical procedure is to introduce the needle inside the foramen, being this step the most difficult for the surgeon. The needle tip must be close to the nerve, but the location of the nerve is not known in advance, so once inside the foramen, the surgeon checks the target adjusting the stimulation potential with the patient's feedback. A second aspect to consider is needle bending during the insertion since, in that case, the tracking system will not show the actual trajectory of the needle. During the experiment, an operator verified that the needle was held still and not bent, and this should be ensured during a clinical procedure. Finally, soft tissue deformation could be a limitation while performing the insertion. The target is the foramen orifice (bone tissue), but the reference marker is located on the patient's skin. This did not influence our phantom experiment as the reference marker was attached to a solid structure of the phantom but could be an issue in the clinical setting.

Regarding insertion time, experienced users were significantly slower and performed a higher number of insertions in comparison with inexperienced participants. Experienced users know that performing shorter insertions involves less suffering for the patient, although it may take longer times or more punctures to reach the target foramen. Additionally, the metrics when using navigation show a lower interquartile range, indicating that the variability between surgeons is reduced, as they achieve similar results no matter the patient or the target.

Actual SNS training methodologies are only based on theoretical lectures combined with surgical procedures where trainee physicians participate as passive spectators. When practical lessons are offered, they are limited to performing the procedure in animal models. For that reason, we believe the proposed simulation software and the manufactured phantom could be easily adapted for low-cost training, teaching professionals SNS needle insertion without involving animal experiments. Additionally, making the source code for our training software available will facilitate medical training in procedures where x-ray projections are needed without radiation risks for the user.

5. Conclusions

In conclusion, we have shown two navigation alternatives based on traditional tracking systems and AR technology that could improve surgical outcomes by significantly reducing needle insertions, surgical time and patient's pain in SNS procedures. To evaluate and compare the two alternatives with a realistic simulation of the clinical procedure, twelve physicians performed several needle insertion tasks on the same realistic setup. We believe that these solutions are feasible to replace current SNS clinical procedures, although AR technology still needs to be improved to be a practical solution in the clinical scenario. Meanwhile, we offer the simulation software to facilitate SNS training.

Declaration of Competing Interest

The authors declare that they have no known competing financial interests or personal relationships that could have appeared to influence the work reported in this paper.

Acknowledgments

Research supported by projects PI18/01625 and AC20/00102 (Ministerio de Ciencia, Innovación y Universidades, Instituto de Salud Carlos III, Asociación Española Contra el Cáncer and European Regional Development Fund "Una manera de hacer Europa"), IND2018/TIC-9753 (Comunidad de Madrid) and project PerPlanRT (ERA Permed). Funding for APC: Universidad Carlos III de Madrid (Read & Publish Agreement CRUE-CSIC 2022).

Supplementary materials

Supplementary material associated with this article can be found, in the online version, at doi:10.1016/j.cmpb.2022.106991.

References

[1] H.B. Goldman, J.C. Lloyd, K.L. Noblett, M.P. Carey, J.C. Castaño Botero, J.B. Gajewski, P.A. Lehur, M.M. Hassouna, K.E. Matzel, I.M. Paquette, S. de Wachter, M.J. Ehlert, E. Chartier-Kastler, S.W. Siegel, International continence society best practice statement for use of sacral neuromodulation, Neurourol. Urodyn. 37 (2018) 1823–1848, doi:10.1002/nau.23515.
[2] E.R. Williams, S.W. Siegel, Procedural techniques in sacral nerve modulation, Int. Urogynecol. J. 21 (2010) 453–460, doi:10.1007/s00192-010-1280-4.
[3] E. Ganio, A.R. Luc, G. Clerico, M. Trompetto, Sacral nerve stimulation for treatment of fecal incontinence: a novel approach for intractable fecal incontinence, Dis. Colon Rectum 44 (2001) 619–631, doi:10.1007/BF02234555.
[4] M.A. Banakhar, T. Al-Shaiji, M. Hassouna, Sacral neuromodulation and refractory overactive bladder: an emerging tool for an old problem, Ther. Adv. Urol. 4 (2012) 179–185, doi:10.1177/1756287212445179.
[5] U. Jonas, C.J. Fowler, M.B. Chancellor, M.M. Elhilali, M. Fall, J.B. Gajewski, V. Grünewald, M.M. Hassouna, U. Hombergh, R. Janknegt, P.E. van Kerrebroeck, A.A. Lylcklama a Nijeholt, S.W. Siegel, R.A. Schmidt, Efficacy of sacral nerve stimulation for urinary retention: results 18 months after implantation, J. Urol. 165 (2001) 15–19, doi:10.1097/00005392-200101000-00004.
[6] S.A. Pilkington, C. Emmett, C.H. Knowles, J. Mason, Y. Yiannakou, Pelvic floor Society, Surgery for constipation: systematic review and practice recommendations, Colorectal Dis. 19 (2017) 92–100, doi:10.1111/codi.13780.
[7] C. Arman, S. Naderi, A. Kiray, F.T. Aksu, H.S. Yilmaz, S. Tetik, E. Korman, The human sacrum and safe approaches for screw placement, J. Clin. Neurosci. Official J. Neurosurg. Soc. Australas. 16 (2009) 1046–1049, doi:10.1016/j.jocn.2008.07.081.
[8] T.C. Chai, G.J. Mamo, Modified techniques of S3 foramen localization and lead implantation in S3 neuromodulation, Urology 58 (2001) 786–790, doi:10.1016/s0090-4295(01)01326-7.
[9] K.E. Husk, L.D. Norris, M.G. Willis-Gray, K.M. Borawski, E.J. Geller, Variation in bony landmarks and predictors of success with sacral neuromodulation, Int. Urogynecol. J. 30 (2019) 1973–1979, doi:10.1007/s00192-019-03883-3.
[10] K.E. Matzel, E. Chartier-Kastler, C.H. Knowles, P.A. Lehur, A. Muñoz-Duyos, C. Ratto, M.B. Rydningen, M. Sørensen, P. van Kerrebroeck, S. de Wachter, Sacral neuromodulation: standardized electrode placement technique, Neuromodulation 20 (2017) 816–824 Technology at the Neural Interface, doi:10.1111/ner.12695.
[11] C.P. Chung, P.A. Neese, H.K. Le, E.T. Bird, Computed tomography-guided S3 lead placement for sacral neuromodulation, Int. Urogynecol. J. 24 (2013) 349–351, doi:10.1007/s00192-012-1816-x.
[12] T. Meissnitzer, S. Trubel, R. Posch-Zimmermann, M.W. Meissnitzer, CT-guided lead placement for selective sacral neuromodulation to treat lower urinary tract dysfunctions, Am. J. Roentgenol. 205 (2015) 1139–1142, doi:10.2214/AJR.14.14270.
[13] P.A. Hellström, J. Katisko, P. Finnilä, M.H. Vaarala, Sacral nerve stimulation lead implantation using the o-arm, BMC Urol. 13 (2013) 48, doi:10.1186/1471-2490-13-48.

[14] J. Castillo, L. Cristóbal, J. Alonso, R. Martín, D. Suárez, M.A. Martínez, C. Cagigas, M. Gómez-Ruiz, M. Gómez-Fleitas, A. Vázquez-Barquero, Sacral nerve stimulation lead implantation in partial sacral agenesis using intra-operative computerized tomography, Colorectal Dis. 18 (2016) O330–O333, doi:10.1111/codi.13437.
[15] D. Mendelsohn, J. Strelzow, N. Dea, N.L. Ford, J. Batke, A. Pennington, K. Yang, T. Ailon, M. Boyd, M. Dvorak, B. Kwon, S. Paquette, C. Fisher, J. Street, Patient and surgeon radiation exposure during spinal instrumentation using intraoperative computed tomography-based navigation, Spine J. 16 (2016) 343–354, doi:10.1016/j.spinee.2015.11.020.
[16] J. Zhang, P. Zhang, L. Wu, J. Su, J. Shen, H. Fan, X. Zhang, Application of an individualized and reassemblable 3D printing navigation template for accurate puncture during sacral neuromodulation, Neurourol. Urodyn. 37 (2018) 2776–2781, doi:10.1002/nau.23769.
[17] Z. Cui, Z. Wang, G. Ye, C. Zhang, G. Wu, J. Lv, A novel three-dimensional printed guiding device for electrode implantation of sacral neuromodulation, Colorectal Dis. 20 (2018) O26–O29 The Official Journal of the Association of Coloproctology of Great Britain and Ireland, doi:10.1111/codi.13958.
[18] I. Rubio-Pérez, A. Díaz Lantada, Surgical planning of sacral nerve stimulation procedure in presence of sacral anomalies by using personalized polymeric prototypes obtained with additive manufacturing techniques, Polymers 12 (2020) (Basel), doi:10.3390/polym12030581.
[19] J. Krücker, S. Xu, N. Glossop, A. Viswanathan, J. Borgert, H. Schulz, B.J. Wood, Electromagnetic tracking for thermal ablation and biopsy guidance: clinical evaluation of spatial accuracy, J. Vasc. Interv. Radiol. 18 (2007) 1141–1150, doi:10.1016/j.jvir.2007.06.014.
[20] G. Turtulici, D. Orlandi, G. Dedone, G. Mauri, A. Fasciani, R. Sirito, E. Silvestri, Ultrasound-guided transvaginal radiofrequency ablation of uterine fibroids assisted by virtual needle tracking system: a preliminary study, Int. J. Hyperth. 35 (2018) 97–104, doi:10.1080/02656736.2018.1479778.
[21] S.W. Wong, A.U. Niazi, K.J. Chin, V.W. Chan, Real-time ultrasound-guided spinal anesthesia using the SonixGPS® needle tracking system: a case report, Can. J. Anaesth. J. Can. Anesth. 60 (2013) 50–53, doi:10.1007/s12630-012-9809-2.
[22] B.J. Park, S.J. Hunt, C. Martin, G.J. Nadolski, B.J. Wood, T.P. Gade, Augmented and mixed reality: technologies for enhancing the future of IR, J. Vasc. Interv. Radiol. 31 (2020) 1074–1082, doi:10.1016/j.jvir.2019.09.020.
[23] R. Rahman, M.E. Wood, L. Qian, C.L. Price, A.A. Johnson, G.M. Osgood, Head-mounted display use in surgery: a systematic review, Surg. Innov. 27 (2020) 88–100, doi:10.1177/1553350619871787.
[24] R. Hecht, M. Li, Q.M.B. de Ruiter, W.F. Pritchard, X. Li, V. Krishnasamy, W. Saad, J.W. Karanian, B.J. Wood, Smartphone augmented reality CT-based platform for needle insertion guidance: a phantom study, Cardiovasc. Interv. Radiol. 43 (2020) 756–764, doi:10.1007/s00270-019-02403-6.
[25] T. Kuzhagaliyev, N.T. Clancy, M. Janatka, K. Tchaka, F. Vasconcelos, M.J. Clarkson, K. Gurusamy, D.J. Hawkes, B. Davidson, D. Stoyanov, Augmented reality needle ablation guidance tool for irreversible electroporation in the pancreas, in: Proceedings of the SPIE, 2018, doi:10.1117/12.2293671.
[26] R. López-Velazco, D. García-Mato, G. Rodríguez-Lozano, M. García-Sevilla, E. Marinetto, D. García-Olmo, M. Desco, M. Ortega-López, J. Pascau, Image guidance for sacral neuromodulation, in: Proceedings of the 31st International Congress and Exhibition Barcelona, Spain, June 20-24, Barcelona, Spain, 2017, pp. 105–106, doi:10.1007/s11548-017-1588-3.
[27] A. Lasso, T. Heffter, A. Rankin, C. Pinter, T. Ungi, G. Fichtinger, PLUS: open-source toolkit for ultrasound-guided intervention systems, IEEE Trans. Biomed. Eng. 61 (2014) 2527–2537, doi:10.1109/TBME.2014.2322864.
[28] J. Tokuda, G.S. Fischer, X. Papademetris, Z. Yaniv, L. Ibanez, P. Cheng, H. Liu, J. Blevins, J. Arata, A.J. Golby, T. Kapur, S. Pieper, E.C. Burdette, G. Fichtinger, C.M. Tempany, N. Hata, OpenIGTLink: an open network protocol for image-guided therapy environment, Int. J. Med. Robot. 5 (2009) 423–434, doi:10.1002/rcs.274.
[29] K.S. Arun, T.S. Huang, S.D. Blostein, Least-squares fitting of two 3-D point sets, IEEE Trans. Pattern Anal. Mach. Intell. (1987) 698–700 PAMI-9, doi:10.1109/TPAMI.1987.4767965.
[30] L. Levine, M. Levine, DRRGenerator: a three-dimensional slicer extension for the rapid and easy development of digitally reconstructed radiographs, J. Clin. Imaging Sci. 10 (2020) 69, doi:10.25259/JCIS_105_2020.
[31] R. Moreta-Martinez, D. García-Mato, M. García-Sevilla, R. Pérez-Mañanes, J.A. Calvo-Haro, J. Pascau, Combining augmented reality and 3D printing to display patient models on a smartphone, J. Vis. Exp. (2020), doi:10.3791/60618.
[32] P. Virtanen, R. Gommers, T.E. Oliphant, M. Haberland, T. Reddy, D. Cournapeau, E. Burovski, P. Peterson, W. Weckesser, J. Bright, S.J. van der Walt, M. Brett, J. Wilson, K.J. Millman, N. Mayorov, A.R.J. Nelson, E. Jones, R. Kern, E. Larson, C.J. Carey, I. Polat, Y. Feng, E.W. Moore, J. VanderPlas, D. Laxalde, J. Perktold, R. Cimrman, I. Henriksen, E.A. Quintero, C.R. Harris, A.M. Archibald, A.H. Ribeiro, F. Pedregosa, P. van Mulbregt, A. Vijaykumar, A. Pietro Bardelli, A. Rothberg, A. Hilboll, A. Kloeckner, A. Scopatz, A. Lee, A. Rokem, C.N. Woods, C. Fulton, C. Masson, C. Häggström, C. Fitzgerald, D.A. Nicholson, D.R. Hagen, DV Pasechnik, E. Olivetti, E. Martin, E. Wieser, F. Silva, F. Lenders, F. Wilhelm, G. Young, G.A. Price, G.-L. Ingold, G.E. Allen, G.R. Lee, H. Audren, I. Probst, J.P. Dietrich, J. Silterra, J.T. Webber, J. Slavič, J. Nothman, J. Buchner, J. Kulick, J.L. Schönberger, J.V. de Miranda Cardoso, J. Reimer, J. Harrington, J.L.C. Rodríguez, J. Nunez-Iglesias, J. Kuczynski, K. Tritz, M. Thoma, M. Newville, M. Kümmerer, M. Bolingbroke, M. Tartre, M. Pak, N.J. Smith, N. Nowaczyk, N. Shebanov, O. Pavlyk, P.A. Brodtkorb, P. Lee, R.T. McGibbon, R. Feldbauer, S. Lewis, S. Tygier, S. Sievert, S. Vigna, S. Peterson, S. More, T. Pudlik, T. Oshima, T.J. Pingel, T.P. Robitaille, T. Spura, T.R. Jones, T. Cera, T. Leslie, T. Zito, T. Krauss, U. Upadhyay, Y.O. Halchenko, Y. Vázquez-Baeza, S. 1. 0 Contributors, SciPy 1.0: fundamental algorithms for scientific computing in Python, Nat. Methods 17 (2020) 261–272, doi:10.1038/s41592-019-0686-2.
[33] A. Elmi-Terander, G. Burström, R. Nachabé, M. Fagerlund, F. Ståhl, A. Charalampidis, E. Edström, P. Gerdhem, Augmented reality navigation with intraoperative 3D imaging vs fluoroscopy-assisted free-hand surgery for spine fixation surgery: a matched-control study comparing accuracy, Sci. Rep. 10 (2020) 707, doi:10.1038/s41598-020-57693-5.
[34] F.A. Mettler, W. Huda, T.T. Yoshizumi, M. Mahesh, Effective doses in radiology and diagnostic nuclear medicine: a catalog, Radiology 248 (1) (2008) 254–263.
[35] D. García-Mato, R. Moreta-Martinez, M. García-Sevilla, S. Ochandiano, R. García-Leal, R. Pérez-Mañanes, J.A. Calvo-Haro, J.I. Salmerón, J. Pascau, Augmented reality visualization for craniosynostosis surgery, Comput. Methods Biomech. Biomed. Eng. Imaging Vis. (2020) 1–8, doi:10.1080/21681163.2020.1834876.
[36] R. Moreta-Martinez, A. Pose-Díez-de-la-Lastra, J.A. Calvo-Haro, L. Mediavilla-Santos, R. Pérez-Mañanes, J. Pascau, Combining augmented reality and 3D printing to improve surgical workflows in orthopedic oncology: smartphone application and clinical evaluation, Sensors 21 (2021) 1370, doi:10.3390/s21041370.
[37] M. García-Sevilla, R. Moreta-Martinez, D. García-Mato, A. Pose-Diez-de-la-Lastra, R. Pérez-Mañanes, J.A. Calvo-Haro, J. Pascau, Augmented reality as a tool to guide PSI placement in pelvic tumor resections, Sensors 21 (2021) 7824, doi:10.3390/s21237824.
[38] C.M. Andrews, A.B. Henry, I.M. Soriano, M.K. Southworth, J.R. Silva, Registration techniques for clinical applications of three-dimensional augmented reality devices, IEEE J. Transl. Eng. Health Med. 9 (2020) 4900214, doi:10.1109/JTEHM.2020.3045642.
[39] Microsoft HoloLens 2, (n.d.). https://www.microsoft.com/en-us/hololens (accessed September 21, 2021).
[40] C. Uhl, J. Hatzl, K. Meisenbacher, L. Zimmer, N. Hartmann, D. Böckler, Mixed-Reality-Assisted Puncture of the Common Femoral Artery in a Phantom Model, J. Imaging 8 (2022) 47, doi:10.3390/jimaging8020047.
[41] C.A. Molina, N. Theodore, A.K. Ahmed, E.M. Westbroek, Y. Mirovsky, R. Harel, E. Orru', M. Khan, T. Witham, D.M. Sciubba, Augmented realityassisted pedicle screw insertion: a cadaveric proof-of-concept study, J. Neurosurg Spine SPI. 31 (2019) 139146, doi:10.3171/2018.12.SPINE181142.
[42] B.J. Park, S.J. Hunt, G.J. Nadolski, T.P. Gade, Augmented reality improves procedural efficiency and reduces radiation dose for CT-guided lesion targeting: a phantom study using HoloLens 2, Sci. Rep. 10 (2020) 18620, doi:10.1038/s41598-020-75676-4.
[43] M. Farshad, P. Fürnstahl, J.M. Spirig, First in man *in-situ* augmented reality pedicle screw navigation, N. Am. Spine Soc. J. (NASSJ) 6 (2021) 100065, doi:10.1016/j.xnsj.2021.100065.
[44] L. Groves, N. Li, T.M. Peters, E.C.S. Chen, Towards a first-person perspective mixed reality guidance system for needle interventions, J. Imaging 8 (7) (2022), doi:10.3390/jimaging8010007.
[45] M. Li, R. Seifabadi, D. Long, Q. de Ruiter, N. Varble, R. Hecht, A.H. Negussie, V. Krishnasamy, S. Xu, B.J. Wood, Smartphone- versus smartglasses-based augmented reality (AR) for percutaneous needle interventions: system accuracy and feasibility study, Int. J. Comput. Assist. Radiol. Surg. 15 (2020) 1921–1930, doi:10.1007/s11548-020-02235-7.
[46] C. Uhl, J. Hatzl, K. Meisenbacher, L. Zimmer, N. Hartmann, D. Böckler, Mixed-reality-assisted puncture of the common femoral artery in a phantom model, J. Imaging 8 (2022) 47, doi:10.3390/jimaging8020047.
[47] R. Moreta-Martinez, M. García-Sevilla, D. García-Mato, A. Pose-Diaz-de-la-Lastra, I. Rubio-Pérez, J. Pascau, Smartphone-based augmented reality system for needle insertion guidance in sacral nerve stimulation, in: Proceedings of the 35th International Congress and Exhibition Munich, Germany, June 21-25, 2021, pp. 103–104, doi:10.1007/s11548-021-02375-4.
[48] T. Song, C. Yang, O. Dianat, E. Azimi, Endodontic guided treatment using augmented reality on a head-mounted display system, Healthc. Technol. Lett. 5 (2018) 201–207, doi:10.1049/htl.2018.5062.